Eur. Phys. J. E **17**, 29–35 (2005)
DOI 10.1140/epje/i2004-10102-5

THE EUROPEAN PHYSICAL JOURNAL E

Anisotropic elastic properties of microtubules

J.A. Tuszyński[1,a], T. Luchko[1], S. Portet[2], and J.M. Dixon[3]

[1] Department of Physics, University of Alberta, Edmonton, Alberta, Canada T6G 2J1
[2] Room 1060, The Samuel Lunenfeld Research Institute, Mount Sinai Hospital, 600 University Avenue, Toronto, Ontario, Canada M5G 1X5
[3] Department of Physics, University of Warwick, Coventry, CV4 7AL, United Kingdom

Received 23 July 2004 and Received in final form 20 December 2004 /
Published online: 6 April 2005 –

Abstract. We review and model the experimental parameters which characterize elastic properties of microtubules. Three macroscopic estimates are made of the anisotropic elastic moduli, accounting for the molecular forces between tubulin dimers: for a longitudinal compression of a microtubule, for a lateral force and for a shearing force. These estimates reflect the anisotropies in these parameters observed in several recent experiments.

PACS. 36.20.-r Macromolecules and polymer molecules – 87.16.Ka Filaments, microtubules, their networks, and supramolecular assemblies

1 Introduction

The cytoskeleton is composed of three different types of filaments organized in networks: microfilaments (MF), intermediate filaments (IF) and microtubules (MT). Each of them has specific physical properties and structures suitable for their role in the cell. For example, the two-dimensional arrangement of MFs in contractile fibers, so-called stress fibers, appears to form cable-like structures involved in the maintenance of the cell shape and transduction pathways. F-actin can support large stresses without a great deal of deformation and it ruptures at approximatively $3.5\,\mathrm{N/m^2}$ [1]. IFs have a rope-like structure composed of fibrous proteins consisting of two coiled coils and are mainly involved in the maintenance of cell shape and integrity. Ma *et al.* [2] shows that IFs resist high applied pressures by increasing their stiffness. They can withstand higher stresses than the other two components without damage [1].

MTs are long hollow cylindrical objects made up of 12 to 17 protofilaments under *in vitro* conditions, and typically of 13 protofilaments *in vivo*. Protofilaments consist of α-, β-tubulin heterodimers longitudinally arranged. Each protofilament is shifted lengthwise with respect to its neighbor describing left-handed helical pathways around the MT. MTs are involved in a number of functions of the cell such as cell shape maintenance, mitosis and they play an important role in intracellular transport. By biological standards, MTs are rigid polymers with a large persistence length of 6 mm [3]. From Jamney's experiments [1], MTs suffer a larger strain for a small stress compared to either MFs or IFs. The rupture stress for MTs is very small and typically is about 0.4–$0.5\,\mathrm{N/m^2}$ [1]. The lateral contacts between tubulin dimers in neighboring protofilaments have a decisive role for MT stability, rigidity and architecture [4]. Tubulin dimers are relatively strongly bound in the longitudinal direction (along protofilaments), while the lateral interaction between protofilaments is much weaker [5].

There have been a number of experimental studies in recent years dealing with the various aspects of the elasticity of MTs. Section 2 summarizes in detail the results of experimental investigations. On the other hand, theoretical effort in this area has been much more limited. For example Jánosi *et al.* [6] have studied the elastic properties of MT tips and walls and the various shapes observed from electron micrographs have been shown to be consistent with their simple mechanical model. However, their model deals chiefly with the geometrical characteristics of MTs and not with their anisotropic properties which is the focus of our effort. The limited flexibility of inter-protofilament bonds in MTs, assembled from pure tubulin, has also been investigated by Chrétien *et al.* [7] via moiré patterns in cytoskeletal micrographs. The position of tubulin subunits and their arrangement on the MT surface enables the moiré period to be predicted.

In this paper we discuss the elastic properties of MTs. In particular we try to utilize the experimental data found in the literature for our theoretical estimations. Our starting point is a review of the information found in the literature regarding the results of experiment and theoretical

[a] e-mail: jtus@phys.ualberta.ca

models of elastic properties of MTs. Using recently published information regarding dimer-dimer interactions and the molecular geometry of the MT, we provide estimates of the elastic moduli accounting for the anisotropy of the MT filament.

2 Elastic parameter review

The response of a cylinder of length L and cross-sectional area A, to an extensional force (stretching), F, is described by *Young's modulus*, $\mathcal{Y}$, and the relationship between these physical quantities is given by Hooke's law,

$$\frac{F}{A} = \mathcal{Y}\frac{\Delta L}{L}, \tag{1}$$

where ΔL is the small length change and the relative extension, $\frac{\Delta L}{L}$, is the unidirectional strain along the direction of the force applied to the cylinder.

Another elastic property is characterized by the *shear* or *twisting modulus*, G, that is expressed, for a homogeneous isotropic material, by [5]

$$G = \frac{\mathcal{Y}}{2(1+\nu)}\,, \tag{2}$$

where ν is Poisson's ratio, representing the relative magnitude of transverse-to-longitudinal strain and its value typically lies in the range $0 < \nu < 0.5$.

Another indicator of the elastic property of a solid is the parameter called *flexural rigidity*, κ_f, that determines the resistance of a filament to a bending force. The higher the flexural rigidity, the greater the resistance to bending. The flexural rigidity is completely determined by the properties of the bonds between the atoms within each protein subunit and the properties of the bonds that hold the subunits together in MTs. For isotropic and homogeneous materials, the flexural rigidity, κ_f, can be represented as the product of two terms (characterizing material properties and their shape), by

$$\kappa_f = \mathcal{Y}\mathcal{I}_y\,, \tag{3}$$

where $\mathcal{I}_y$ is a shape-dependent parameter called the second moment of inertia. For a hollow cylinder [8,3] it is given by $\mathcal{I}_y = \pi(R_o^4 - R_i^4)/4$, where R_o and R_i are the outer and the inner radii, respectively. However, for a hollow cylinder made up of n cylindrical protofilaments, where each protofilament has radius r, $\mathcal{I}_y$ is given by $\mathcal{I}_y = \left(\frac{2}{\pi^2}n^3 + n\right)\frac{\pi}{4}r^4$ [8].

The *persistence length*, ξ_p, is another index which describes the filament's resistance to thermal forces. Roughly speaking this length is the distance over which a filament appears straight and can be expressed by

$$\xi_p = \frac{\kappa_f}{k_B T} = \frac{\mathcal{Y}\mathcal{I}_y}{k_B T}\,, \tag{4}$$

where k_B is Boltzmann's constant and T is the temperature in Kelvin. The more flexible the filament, the smaller the persistence length. Polymers for which persistence length and contour length are similar are called semiflexible polymers.

Table 1. Experimental data for elastic properties of MTs (and other proteins) from the literature.

Young's modulus, $\mathcal{Y}$	(1.2–2.7) $\times 10^9\,\mathrm{N/m^2}$	[8–11]
	(1–5) $\times 10^8\,\mathrm{N/m^2}$	[5,12]
Shear modulus, G	$1.4\,\mathrm{N/m^2}$	[13]
	$10^3\,\mathrm{N/m^2}$ between MTs	[10]
	$34\,\mathrm{N/m^2}$ gel (concentr.-dependent)	[1]
	$1.4\times 10^6\,\mathrm{N/m^2}$ at 25 °C (temp.-dependent)	[5]
Flexural rigidity, κ_f	(16–45) $\times 10^{-24}\,\mathrm{N\,m^2}$	[14–17,8,18–20]
	(2.9–5.1) $\times 10^{-24}\,\mathrm{N\,m^2}$	[21]
Poisson's ratio, ν	0.3 for macromolecules	[22,12]
	0.4 for MFs	[11]
Persistence length, ξ_p	(1–6.3) $\times 10^{-3}$ m	[3,15,16]

In Table 1 we list the different values found in the literature for the above-defined parameters for MTs. From Table 1 we observe that the shear and Young's moduli are significantly different. This observation describes an anisotropic material. Hence, MTs are inhomogeneous and anisotropic. The bending deformation and stretching of filaments are governed by Young's modulus and the sliding between filaments is governed by the shear modulus [5]. Note that the values of the shear modulus, G, seem to be strongly dependent on the experimental conditions and show little consistency, as we will attempt to elucidate in Section 4.

3 Estimation of tubulin-tubulin interactions

Tubulin was first imaged to atomic resolution in 1998 [23], following 30 years of difficult work by a number of labs with this protein. Nogales *et al.* published the structure of α- and β-tubulin which were co-crystallized in the heterodimeric form [23]. Electron diffraction was performed for tubulin assemblies in the form of zinc sheets. The work establishes that the structures of α- and β-tubulin are nearly identical and confirms the consensus speculation. A detailed examination shows that each monomer is formed by a core of two β-sheets that are surrounded by α-helices. The monomer structure is very compact, but can be divided into three functional domains: the amino-terminal domain containing the nucleotide-binding region, an intermediate domain containing the taxol-binding site, and the flexible carboxy-terminal domain.

Using the refined tubulin crystal structure produced by Löwe *et al.* [24], Sept *et al.* [25,26] calculated the

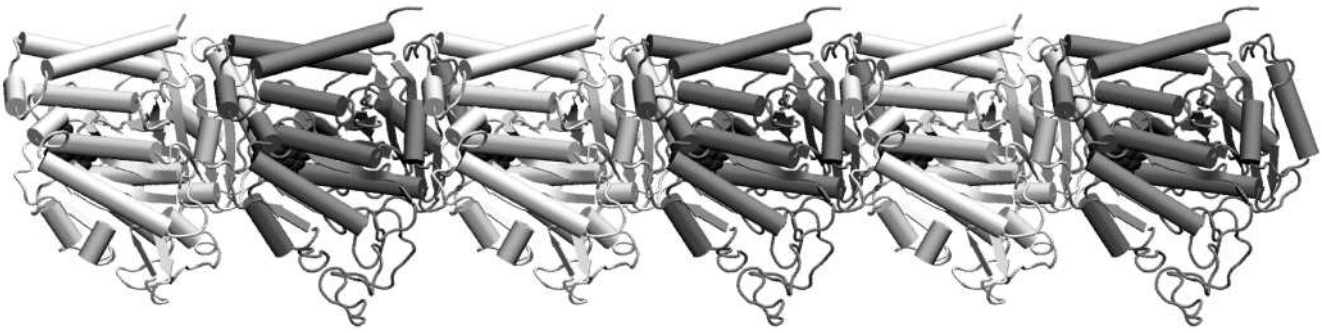

Fig. 1. MT protofilament. α and β monomers are colored gray and white, respectively. Image created with VMD [27].

protofilament-protofilament energy as a function of the shift along the protofilament axis. Two protofilaments were constructed similar to Figure 1 and translated relative to each other along the MT axis. Using Poisson-Boltzmann calculations and a surface area term the interaction energy was computed over a 80 Å translation in 2 Å steps. The data published in this work indicate the presence of two stable equilibrium positions that clearly correspond to the known MT lattice types A and B.

In fact, a recent paper by VanBuren *et al.* [28] estimated the values of lateral and longitudinal bond energies in an MT structure using a stochastic model of assembly dynamics. Their analysis predicts the lateral bond energy to be in the range from -2.2 to -5.7 kT (which translates to -9.1×10^{-21} to -2.4×10^{-20} J) while the longitudinal bond energy is given from -6.8 to -9.4 kT (-2.8×10^{-20} to -3.9×10^{-20} J). However, without the knowledge of the potential's positional dependence these values cannot provide information on the corresponding elastic coefficients.

Using this potential map (Sept *et al.*, Fig. 1 [26]) we have evaluated the corresponding elastic coefficient in a harmonic approximation around the potential minimum. We found the value $k \approx 4\,\mathrm{N/m}$ which will be used in the next section. Note that an early phenomenological estimate of the spring constant k [19] was approximately 40 times smaller and predicted incorrectly that the rigidity of MTs is 100 times lower than that of actin. Unfortunately, still no results are available at present which would give the values of the elastic coefficients along different directions and not just as the result of protofilament-protofilament shifting along the MT axis as demonstrated in Sept *et al.* [25,26]. While this calculation imposes a computational challenge, it is only a matter of time before these values are obtained in a subsequent calculation of MTs anisotropic elastic properties.

Recently, De Pablo *et al.* have estimated experimentally by radial indentation of MTs with a scanning force microscope tip a spring constant value related to radial interactions between neighboring protofilaments [29]. Indentations, induced by the nanometer-sized tip positioned on the top of an MT, result in a linear elastic response with the spring constant $\tilde{k} = 0.1\,\mathrm{N/m}$. Clearly, $\tilde{k} \ll k$. Tubulin dimers are relatively strongly bound in the longitudinal direction (along protofilaments), while the lateral interaction between protofilaments is much weaker [5,30,

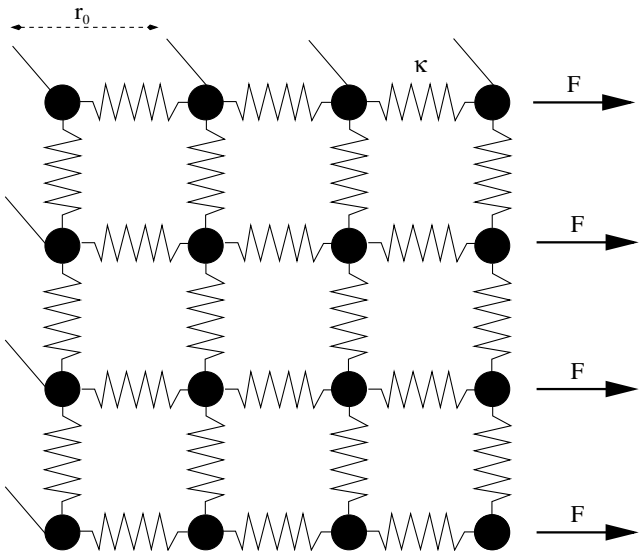

Fig. 2. A cubic lattice of particles separated by r_0 when in equilibrium, connected by elastic springs with spring constants κ and subjected to a force F [8].

26]. Hence, if we define κ_p as the elastic constant between the two dimers along a protofilament, and κ_l as the elastic constant between the two dimers belonging to adjacent protofilaments, then $\kappa_p > \kappa_l = k$.

An order of magnitude estimate of this particular elastic constant, κ_l, can be found in [19] which, when units are converted, results in $\kappa_l = 0.1\,\mathrm{N/m}$. This compares very well with the value given above based on the experiment reported in [29].

4 Estimate of anisotropic elastic properties from molecular forces

In this section we will make estimates of the anisotropic elastic moduli measured for individual MTs based on the internal geometry of the MT and the molecular forces acting between individual dimers. To give a simple conceptual example we follow [8] and imagine a perfect cubic lattice connected by springs, see Figure 2.

Suppose a force F is applied along the line of springs as indicated in Figure 2. Each bond experiences this force

which is perpendicular to one side of the lattice. Each spring will be extended by a small distance Δr, from its equilibrium state r_0, according to the application of Hooke's law to a spring *i.e.* $F = \kappa \Delta r$. Dividing this relation through by r_0^2 we obtain

$$\frac{F}{r_0^2} = \frac{\kappa}{r_0}\frac{\Delta r}{r_0}. \tag{5}$$

The left-hand side of equation (5) represents the force per unit area or stress whereas $\frac{\Delta r}{r_0}$ on the right-hand side, deformation per unit length, describes the strain involved. From equation (1), we therefore obtain Young's modulus of this material as $\mathcal{Y} = \frac{\kappa}{r_0}$. In essence the value of Young's modulus is proportional to the spring constant which depends on the strength of the intermolecular forces. It is inversely proportional to the equilibrium separation between neighboring molecules.

Although the above estimate appears to be rather crude at first sight, it compares quite well to earlier work on polymer elasticity [31] which gives a formula for the Young's modulus of a filamentous polymer

$$\mathcal{Y} = \kappa \frac{r_0}{\pi a^2} \tag{6}$$

with r_0 denoting the centre-to-centre distance between neighboring monomers and a representing the radius of the filament.

Using the same method, we estimate below the effective elastic moduli for a longitudinal, a lateral and a shear deformation (Fig. 3).

4.1 Effective Young's modulus due to longitudinal compression (directed parallel to the protofilament of an MT)

When a compressive force, F, is applied as shown in 1) of Figure 3, there will be a small displacement, Δr_p, of the distance between two dimers of a particular protofilament given by

$$F = \kappa^{\parallel} \Delta r_p \,, \tag{7}$$

where $\kappa^{\parallel}$ is the elastic constant between the two dimers along a protofilament (this was referred to earlier as κ_p). Dividing both sides of equation (7) by the area, A, over which the force is applied we obtain

$$\frac{F}{A} = \frac{\kappa^{\parallel}}{A} \Delta r_p. \tag{8}$$

Suppose N is the number of protofilaments around the MT, then

$$A = \frac{1}{N}\pi(R_o^2 - R_i^2) \tag{9}$$

where R_o and R_i are the outer and the inner radii of the MT, respectively.

Hence, from equations (7–9) we obtain

$$\left(\frac{F}{A}\right) = \frac{N\kappa^{\parallel} l}{\pi(R_o^2 - R_i^2)} \left(\frac{\Delta r_p}{l}\right). \tag{10}$$

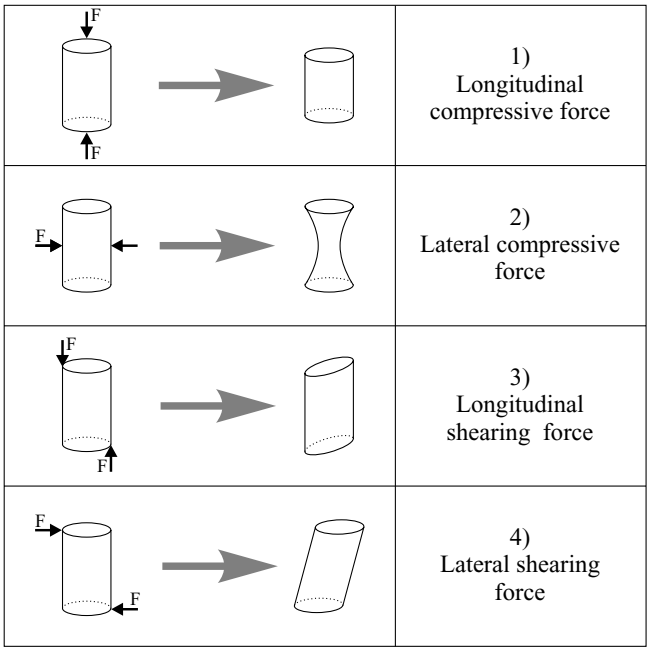

Fig. 3. Different types of forces applied to a cylinder and resulting deformations. 1) A compressive force applied longitudinally to the tip of the filament. 2) A compressive force applied laterally to the wall of a filament. 3) A longitudinal shearing force. 4) A lateral shearing force.

The left-hand side of equation (10) is the stress applied and the term in the brackets on the right, assuming l is the equilibrium distance between dimers, is the strain or incremental displacement per unit length. Hence, from equation (1) the effective Young's modulus, $\mathcal{Y}_{\parallel}$, is given by

$$\mathcal{Y}_{\parallel} = \frac{N\kappa^{\parallel} l}{\pi(R_o^2 - R_i^2)}. \tag{11}$$

We estimate the value of $\kappa^{\parallel}$ to be 4 N/m which is obtained from the harmonic approximation of the interaction energy profile published by Sept *et al.* (see Fig. 1 in [26]). Further, taking $N = 13$, $l = 8\,\text{nm}$, $R_o = 12.5\,\text{nm}$, and $R_i = 7.5\,\text{nm}$, and from equation (11) we find that our estimate of $\mathcal{Y}_{\parallel}$ is $1.32 \times 10^9\,\text{N/m}^2$ [26] which is in very good agreement with the experimental data found in the literature (see Tab. 1).

4.2 Effective elastic modulus due to a lateral force (perpendicular to the protofilament)

In this case (namely, entry 2) of Fig. 3)

$$F = \kappa_{\perp} \Delta r, \tag{12}$$

where Δr is the displacement of dimers in two adjacent protofilaments and $\kappa_{\perp}$ is the elastic constant for the compressive force (see Fig. 4(b)), the experimental value analogous to $\kappa_{\perp}$ has been measured by De Pablo *et al.* [29].

Since there are two adjacent dimers and we need to project the force along the line joining the two dimers, we

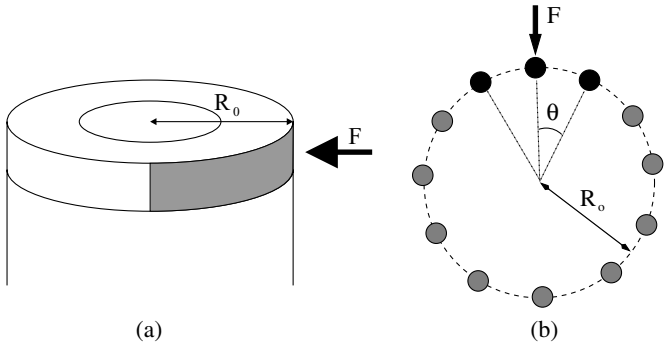

Fig. 4. (a) Side elevation of an MT showing the area in grey to which the force F is applied. (b) Cross-section of an MT showing the direction of the applied force.

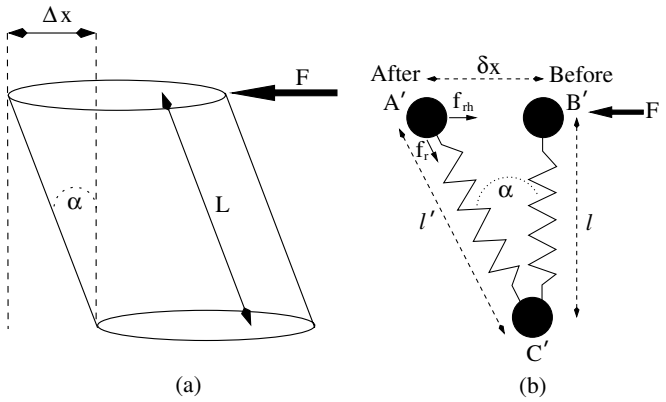

Fig. 5. (a) Section of an MT of length L, subjected to a lateral shearing force, F. (b) Movement of a single dimer as a result of the force F indicating the undisturbed position (before, B') and the position following displacement (after, A').

multiply both sides of equation (12) by $2\sin\theta$, where θ is the angle subtended by 2 adjacent dimers at the center of the MT (see Fig. 4(b)). We then divide the result by an appropriate area (see Fig. 4(a)), A, given by

$$A = \pi R_o l, \tag{13}$$

l being the distance between two neighboring layers (Fig. 4(a)) calculated as a center-to-center distance. Thus,

$$\frac{2F\sin\theta}{A} = \frac{2\kappa_\perp \sin\theta}{\pi l}\left(\frac{\Delta r}{R_o}\right). \tag{14}$$

The part on the left-hand side of equation (14), $2F/A$, represents the applied stress, and putting the left-hand $\sin\theta$ to the right-hand side gives $(\Delta r/R_o \sin\theta)$ as the resultant strain, where $R_o\sin\theta$ is the equilibrium separation of one pair of dimers. Hence, the effective lateral elastic modulus, $\mathcal{Y}_\perp$, is estimated to be given by

$$\mathcal{Y}_\perp = \frac{2\kappa_\perp \sin\theta}{\pi l}. \tag{15}$$

If we use the value of $\kappa_\perp$ as the currently available estimate for the elastic coefficient [29], *i.e.* $\kappa_\perp = 0.1\,\mathrm{N/m}$, $\theta = \frac{\pi}{6}$, and $l = 8\,\mathrm{nm}$ then the corresponding value of the Young's modulus is found to be $\mathcal{Y}_\perp = 4\times10^6\,\mathrm{N/m^2}$. At any rate, due to the presence of the $\sin\theta$ factor in equation (15) and a small value of θ ($\theta = \frac{2\pi}{N-1}$, where N is the number of protofilaments) we expect the Young's modulus to be anisotropic for the parallel and perpendicular directions along which it may differ by as much as an order of magnitude.

4.3 Effective elastic modulus due to a lateral shearing force (see entry 4) in Fig. 3)

The cross-sectional area of the MT is πR_o^2, whereas the length of the section of an MT (see Fig. 5(a)) is $L = nl$ where n is the number of layers of dimers and l the distance between two neighboring layers. The net macroscopic displacement, Δx (see Fig. 5(a)) is obviously given by $\Delta x = n\delta x$, where δx (see Fig. 5(b)) is the microscopic lateral displacement due to the shearing force. With f_r denoting the inter-dimer force (see Fig. 5(b)) between a displaced dimer, A', and a relatively stationary one, C', we have

$$f_r = \kappa_s(l' - l)\,, \tag{16}$$

where κ_s is the microscopic elastic constant and $l' - l$ denotes the change in the interdimer distance (*i.e.* the difference in length between $B'C' = l$ and $A'C' = l'$).

We denote the restoring force across the section of the MT by f_{rh} (see Fig. 5(b)) which, by vectorial addition, is related to the restoring force between dimers A' and C', f_r, by

$$f_{rh} = f_r \sin\alpha. \tag{17}$$

If N is the number of protofilaments around the perimeter of the MT we have

$$\begin{aligned} F = Nf_{rh} &= Nf_r\sin\alpha\,, && \text{from equation (17)}\\ &= N\kappa_s(l'-l)\sin\alpha\,, && \text{from equation (16)}\\ &= N\kappa_s l(\tfrac{1}{\cos\alpha} - 1)\sin\alpha\,, \end{aligned} \tag{18}$$

since it follows from Figure 5b that $l = l'\cos\alpha$. Rearranging equation (18),

$$F = N\kappa_s l(1-\cos\alpha)\tan\alpha \tag{19}$$

and, using the fact that the cross-sectional area is $A = \pi R_o^2$ and $\tan\alpha = \frac{\delta x}{l} = \frac{\Delta x}{L}$, we have

$$\frac{F}{A} = \frac{N}{\pi R_o^2}\kappa_s l(1-\cos\alpha)\frac{\Delta x}{L} = G\left(\frac{\Delta x}{L}\right), \tag{20}$$

where G is the shearing modulus. Hence, we deduce that the shearing modulus can be finally expressed by

$$G = \frac{N}{\pi R_o^2}\kappa_s l(1-\cos\alpha) \simeq \frac{N}{\pi R_o^2}\kappa_s l\frac{\alpha^2}{2}\,, \tag{21}$$

where α is the angle of deformation in radians. We have used the fact that α is small by expanding the cosine. The angle α can lie between the following limits:

$$0.001 \le \alpha \text{ in radians } \le 0.1\,. \tag{22}$$

From equation (21) we see that the shear modulus, G, varies greatly with possible values of α and hence also with the size and magnitude of the displacement. Taking typical values, for example $N = 13$, $l = 8\,\mathrm{nm}$, $R_o = 12.5\,\mathrm{nm}$ and $\kappa_s \approx 0.5\,\mathrm{N/m}$, we find G may vary between the following estimated limits:

$$53\,\mathrm{N\,m^{-2}} \leq G \leq 0.5 \times 10^6\,\mathrm{N\,m^{-2}}\,. \tag{23}$$

Note that the large variation in the value of G found in equation (23) reflects the large differences seen in the various experimental data (see Tab. 1) and may provide an explanation for this diversity. The crucial point to make here is that the deformation angle, α, enters into the shear modulus formula. Combining equations (20) and (21) allows us to calculate the force required for the shearing action as a function of the angle, α. For example, with the use of typical structural parameters and for $\alpha = 0.1$ the shearing force amounts to more than 20 pN which is quite significant. While the computer simulations of Sept *et al.* [26] addressed the problem of longitudinal shearing forces (see entry 3) in Fig. 3) and the resulting strain, the currently available experimental techniques are unable to measure these effects. On the other hand, lateral shearing forces and their effects can be tested experimentally with no major difficulties.

5 Discussion

The objective of this paper was to analyze, describe and theoretically estimate the anisotropic elastic properties of MTs. This has been possible due to a recently obtained experimental body of data coming from several groups and describing a number of physical and structural properties of MTs. In order to synthesize the data we reviewed the literature taking into account the geometry of MTs, experimental data, and their extrapolation. The most marked aspect of MTs observed was the anisotropy of the elastic coefficients. This led us to propose a molecular model that explains the bulk values in terms of the molecular protein-protein interactions. By and large the agreement between theory and experiment is satisfactory. An interesting by-product of this calculation was that the shear modulus depends on the magnitude of the deformation whereas Young's moduli due to a longitudinal or lateral force are only dependent on the structure of MTs. Hence the diversity of experimental data may be explained as arising due to different magnitudes of the forces applied. It should be noted that the calculation of the shear modulus, G, defined in equation (21), refers to a completely different physical situation than the one involved in flexural rigidity which is commonly measured experimentally, *e.g.*, using optical tweezers [32]. In the latter case a cantilevered beam is subjected to a force, F, applied to its free tip while the other end is clamped. Take the length of the rod to be L and the free tip to be deflected from the resting configuration by a distance $y(L)$. The basic formula for small-angle deflection is given by $F = \kappa \cdot y(L)$, where the cantilever spring constant κ is given by $\kappa = 3\kappa_f/L^3$ and κ_f, defined in equation (3), is the flexural rigidity of the rod [8]. With the flexural rigidity of an MT estimated as $\kappa_f = 30 \times 10^{-24}\,\mathrm{N\,m^2}$, Gittes *et al.* [17] found that the spring constant of an MT with $L = 10\ \mu$m is approximately $\kappa \simeq 10^{-7}\,\mathrm{N/m}$. Consequently a force of only 1 pN is able to deflect an MT by up to 1μm which is supported by measurements using laser tweezers [8]. However, such large deflections are *not* produced by shearing forces as calculated above. The difference in the physical mechanisms is that shearing forces lead to stacking displacements at right angles to the stack while flexural forces cause a small-angle bending between dimers in adjacent stacks. Clearly, it is easier to bend a filament than to exert a shearing force.

All the theoretical estimates of the molecular spring constants required a knowledge of the tubulin dimer-dimer interaction potential. In Section 3 we discussed in some detail how the estimate of the spring constant was made based on molecular-dynamics simulations or experiments. This is still a major computational challenge that merits an independent study in its own right. Fortunately, the published atomic resolution structure of tubulin afforded us with an opportunity to carry out preliminary molecular-dynamics simulations for this problem that provided only order of magnitude estimates with some degree of confidence. With the knowledge of one particular interaction strength between two neighboring dimers [25,26] as guidance, we have obtained rough estimates of the molecular spring constants along three different directions on the MT surface.

An objection may be raised that due to the fact that an MT is an anisotropic elastic structure, it posesses many more deformation tensor components than those introduced in the present article. In particular elastic coefficients corresponding to the various off-diagonal effects linking forces applied in one direction and deformations in another have not been exhaustively analysed here. This is true and the deformation tensor would in general contain 21 components [33,34]. However, both experimentally and theoretically we are not yet at the stage of being able to estimate many of these off-diagonal components. An MTs' structure is highly anisotropic elastically and hence we expect the direct effects of the application of compressional and tensional forces to be dominant. In our estimates of the continuum elastic coefficients the link was made to the molecular structure and protein-protein interactions. We have used, in addition to geometrical properties of MTs, approximate values for the handful of spring constants describing the dimer-dimer interactions in an MT. Once more detailed molecular-dynamics simulations reveal additional interaction constants we will be able to extend the model to include the remaining tensor components. Alternatively, experimental techniques may be utilized to do measurements of the dispersion relations for the various phonon modes, *e.g.* through Brillouin scattering, which would provide the required information indirectly as is done in the studies of ferroelasticity.

In conclusion, while the gross elastic anisotropic features of MTs are quite well explained with the existing

models and parameter values, still more work is required to obtain a higher level of confidence and excellent quantitative agreement.

This project has been supported by grants from NSERC and MITACS. J.M. Dixon would like to thank the staff and members of the Physics Department of the University of Alberta, for all their kindness and thoughtfulness during his stay. S. Portet was supported by Genome Canada, the Ontario R&D Challenge Fund and the Canadian Institutes of Health Research.

References

1. P.A. Janmey, U. Euteneuer, P. Traub, M. Schliwa, J. Cell Biol. **113**, 155 (1991).
2. L. Ma, J. Xu, P.A. Coulombe, D. Wirtz, J. Biol. Chem. **274**, 19145 (1999).
3. D. Boal, *Mechanics of the Cell* (Cambridge University Press, 2002).
4. P. Meurer-Grob, J. Kasparian, R.H. Wade, Biochemistry **40**, 8000 (2001).
5. A. Kis, S. Kasas, B. Babic, A.J. Kulik, W. Benoit, G.A.D. Briggs, C. Schonenberger, S. Catsicas, L. Forro, Phys. Rev. Lett. **89**, 248101 (2002).
6. I.M. Janosi, D. Chretien, H. Flyvbjerg, Eur. Biophys. J. **27**, 501 (1998).
7. D. Chretien, H. Flyvbjerg, S.D. Fuller, Eur. Biophys. J. **27**, 490 (1998).
8. J. Howard, *Mechanics of Motor Proteins and the Cycloskeleton* (Sinauer Associated Inc., 2001).
9. Dimitrije Stamenovic, Srboljub M. Mijailovich, Iva Marija Tolic-Norrelykke, Jianxin Chen, Ning Wang, Am. J. Physiol. Cell Physiol. **282**, 617 (2002).
10. J.A. Tolomeo, M.C. Holley, Biophys. J. **73**, 2241 (1997).
11. O. Wagner, J. Zinke, P. Dancker, W. Grill, J. Bereiter-Hahn, Biophys. J. **76**, 2784 (1999).
12. Y.M. Sirenko, M.A. Stroscio, K.W. Kim, Phys. Rev. E **53**, 1003 (1996).
13. M. Sato, W.H. Schwartz, S.C. Selden, T.D. Pollard, J. Cell Biol. **106**, 1205 (1988).
14. L. Cassimeris, D. Gard, P.T. Tran, H.P. Erickson, J. Cell Sci. **114**, 3025 (2001).
15. M. Elbaum, D.K. Fygenson, A. Libchaber, Phys. Rev. Lett. **76**, 4078 (1996).
16. D. Kuchnir Fygenson, M. Elbaum, B. Shraiman, A. Libchaber, Phys. Rev. E **55**, 850 (1997).
17. F. Gittes, B. Mickey, J. Nettleton, J. Howard, J. Cell Biol. **120**, 923 (1993).
18. B. Mickey, J. Howard, J. Cell Biol. **130**, 909 (1995).
19. J. Mizushima-Sugano, T. Maeda, T. Miki-Noumura, Biochim. Biophys. Acta **755**, 257 (1983).
20. Francois Nedelec, J. Cell Biol. **158**, 1005 (2002).
21. H. Felgner, R. Frank, M. Schliwa, J. Cell Sci. **109**, 509 (1996).
22. Y.M. Sirenko, M.A. Stroscio, K.W. Kim, Phys. Rev. E **54**, 1816 (1996).
23. E. Nogales, S. Wolf, K. Dowling, Nature **391**, 199 (1998).
24. J. Löwe, H. Li, K. Dowling, E. Nogales, J. Mol. Biol. **313**, 1045 (2001).
25. David Sept, Nathan A. Baker, J. Andrew McCammon, in *46th Annual Meeting of the Biophysical Society, San Fransico, CA, 2002*, Book of Abstracts.
26. David Sept, Nathan A. Baker, J. Andrew McCammon, Protein Sci. **12**, 2257 (2003).
27. W. Humphrey, A. Dalke, K. Schulten, J. Mol. Graph. **14**, 33 (1996) `http://www.ks.uiuc.edu/Research/vmd/`.
28. Vincent VanBuren, David J. Odde, Lynne Cassimeris, Proc. Natl. Acad. Sci. U.S.A. **99**, 6035 (2002).
29. P.J. de Pablo, I.A.T. Schaap, F.C. MacKintosh, C.F. Schmidt, Phys. Rev. Lett. **91**, 098101 (2003).
30. E. Nogales, Cell. Mol. Life Sci. **56**, 133 (1999).
31. F. Ooshawa, S. Asakura (Editors), *The Thermodynamics of the Polymerization of Protein* (Academic Press, London, 1975).
32. M. Kurashi, M. Hoshi, H. Tashiro, Cell Motil. Cytoskeleton **30**, 221 (1995).
33. L.D. Landau, E.M. Lifshitz, L.P. Pitaevshii, *Theory of elasticity*, 3rd edition (Butterworth Heinamann, 1995).
34. M.P. Marder, *Condensed Matter Physics* (John Wiley and Sons, New York, 2000).